Master's Thesis of Engineering

Development of Advanced Raman Visualization Method for Analysis of Smart Structural Binder

고급 라만 시각화기법 개발을 통한 스마트 구조 결합재 연구

February 2023

Graduate School of Civil and Environmental Engineering
Seoul National University
Smart City Engineering Major

Yangwoo Lee

Development of Advanced Raman Visualization Method for Analysis of Smart Structural Binder

Jae-Yeol Cho

Submitting a master's thesis of
Civil and Environmental Engineering
February 2023

Graduate School of Civil and Environmental Engineering
Seoul National University
Smart City Engineering Major

Yangwoo Lee

Confirming the master's thesis written by
Yangwoo Lee
February 2023

Chair _____(Seal)
Vice Chair _____(Seal)
Examiner _____(Seal)

Abstract

The advanced analysis technique of in-situ Raman Imaging for investigating the hydration behavior of structural binder system was studied in this paper. Especially, attempts were made to enable controlling water to cement ratio through surrounding sample with glue gun and coverslip, which has been firstly reported. The hydration of ye'elimite in the presence of gypsum was mainly analyzed by Raman spectroscopy to prove the potential applicability of the proposed technique.

Compared to previous studies conducted by XRD and NMR, amorphous phases such as AFm phases and amorphous aluminum hydroxide phases could be clearly identified. Also, using Raman spectroscopy, saving a lot of time and labor required for in-situ hydration analysis was possible. Furthermore, temporal and spatial interpretation of the in-situ hydration process, which could not be achieved by the conventional analysis method, such as XRD and SEM, became possible. It spatially confirmed the specific position of decomposition of aluminum hydroxide gel phase as well as additional formation of ettringite. This method enables the characterization of heterogeneous and amorphous constituent phases in various time span including early age.

Keyword : Ye'elmite, Calcium SulfoAluminate cement, Raman Spectroscopy, Imaging, Cement Chemistry, In-situ Hydration
Student Number : 2021-28923

Table of Contents

Chapter 1. Introduction

1.1. Study Background

Cement is a widely used in the construction of buildings and infrastructure because of its durability, cost-efficiency and workability and its usage mixed with aggregates has skyrocketed in latest decades.[1] Because of this increase in cement demand, cement manufacturing industry is one of the major source of global industrial emissions, accounting for 26% of total industrial CO2 emissions.[2] The production of Portland cement(PC), the most commonly used cement, emits 0.8-0.9 tons of CO2 per ton of PC worldwide.[3] As reported by the U.S. Geological Survey, 4.2 gigatons of cement are manufactured globally every year, and the percentage of CO2 emissions by cement industry in overall CO2 emissions has nearly doubled from 4% in 1970 to nearly 10%.[4] Thus, the demand for reducing CO2 emissions by cement industry for sustainable development and maintenance is inevitable.

To curtail energy consumption and CO2 emissions in cement industry, there are several actions that the industry can take including 1) improving the energy-efficiency of the cement manufacturing process, 2) developing higher-strength concrete mix designs in order to decreasing the mass of concrete members, 3)

substituting Portland Cement clinker to low-carbon supplementary cementitious materials(SCM), 4) utilizing alternative low-carbon clinkers instead of Portland clinkers. OPC's high kiln temperature (i.e., ~1450 °C) and the decomposition of limestone in the raw materials are the main causes of its significantly high carbon footprint.[5] The high carbon footprint of OPC clinker is mainly due to its high content of alite (C_3S), required in today's concrete market for its rapid early strength gain.[6] To compensate for the high carbon footprint of alite the current industrial trend is to replace more pozzolanic SCMs with the OPC clinker. Pozzolanic SCMs can react with excess lime produced by alite hydration, forming cementitious composite with sufficient strength. These include manufacture of artificial pozzolans such as calcined clays, which are preferably used together with limestone powders due to their chemical synergies. However, a UNEP-supported study[7] showed that the current approaches utilizing SCMs such as slags, fly ashes and natural pozzolans was reaching their limits due to a lack of adequate source of guaranteed quality. Unused, inexpensive SCM sources are mainly coal fly ash with inherently poor quality control, low reactivity, and limited availability.

Against this context, the need for a precise understanding of cement hydration kinetics has increased. Analyzing and

characterizing the chemical and physical composition of cement matrix are crucial to hydration kinetics comprehension and developments in sustainable structural materials.[8] Even though there are considerable efforts to characterize its kinetics using techniques such as X-ray Diffraction(XRD), Nuclear Magnetic Resonance(NMR), and Scanning Electron Microscopy(SEM), quantifying phase composite of cement sample is still in ambiguous stage. Plus, those techniques require pre-processings which prevent in-situ quantification and spatial mapping.

Raman microspectroscopy is a non-destructive technique for identification and analysis, having suitable characteristics for imaging and quantifying the process of early age cement hydration. Raman signal is not interrupted by water or substrate and pre-processings such as milling and hydration stoppage are not required for analysis. And imaging whole system does not take long time of exposure compared to other analysis instruments. Furthermore, the probability of damaging sample is comparatively low since Raman microspectroscopy, utilizing monochromatic wave as an excitation beam. Previous works using Raman spectroscopy to cement research were primarily concentrated on identifying clinker phases in OPC and their hydration products.

Plus, there are not enough studies about early stage cement

hydration regarding eco-friendly clinkers such as ye'elimite.

To interpret the Raman signal, peak intensity, width, and position are mainly considered.[9] However, these approach limits a structure of sample, thus curing condition for sample is also limited. Recent study broadened the border of this limited condition utilizing its own sample mold, enabling catching early stage mapping of OPC and analysis of it.[10] However, the approach adopted in that study also have limitation in the perspective of water to binder ratio. In this study, to enable setting water to binder ratio that researchers want, cost efficient coverslip and glue gun are adopted. To check the potential of this method, complex phenomena of ye'elimite hydration was mapped.

Calcium SulfoAluminate-type cements(CSA), mainly composed of ye'elimite, are attracting attention due to its low manufacturing temperature(~1200℃) compared to OPC(~1400℃), thus its resulting CO2 emission is much lower. Compared to PC, more efforts have to be taken for CSA to develop and to control an appropriate and durable mix design, for instance (1) quantity and reactivity of the calcium sulfate added strongly affects early hydration kinetics and volume stability [11]–[13], (2) early setting often needs to be controlled with admixtures [14], and (3) durability is much less explored [3], [15]. Despite the long history of the CSA

systems use in many applications, the early hydration mechanisms of ye'elimite clinkers are not well understood although the understanding of these mechanisms is very important since the hydration of ye'elimite regulates the evolution of the early cement performance.

In this study, to evaluate potential of given method, the experiment conducted at previous study [16] was reproduced. Early hydration of orthorhombic ye'elimite with gypsum were tracked by means of heat flow calorimetry, XRD, and NMR. Those result was compared with in-situ monitoring and imaging of fresh cement mix conducted by Raman spectroscopy.

Chapter 2. Materials and Methods

2.1 Sample Preparations

Ye'elimite (CTLGroup, Skokie, IL) was used for the experiments. The modification of ye'elimite used in this study is orthorhombic. For Raman data acquisition, 2g of ye'elimite and 1g of gypsum was added to a cup containing 3g of water to make water to cement ratio 1. This amount of water is theoretically sufficient in order to guarantee complete ettringite precipitation according to Eq (1). The cement nomenclature in this paper is following cement chemist notation; $\mathrm{C} = \mathrm{CaO}, \mathrm{S} = \mathrm{SiO_2}, \mathrm{A} = \mathrm{Al_2}O_3, F = Fe_2O_3$ and $H = H_2O$

$$C_4A_3\overline{S} + 2C\overline{S} + 38H \rightarrow C_6A\overline{S}_3H_{32} + 2AH_3 \quad (1)$$

After addition of powder to water, sample was stirred vigorously with metal spoon and spatula for 1 min. Then, sample is moved on the slide glass. For the better mapping, commercially available iron needle was placed as reference. Two iron needles are placed in parallel and cement paste is placed between them. And then, coverslip is placed on the cement paste. The coverslip is pressed slightly to remove possible imbalance in height that causes deterioration in Raman data quality. After compression, glue gun was applied to boundary to prevent possible contamination and evaporation.

2.2 Raman Spectroscopy

Raman spectra and optical images were acquired using a Raman confocal system (Weve, South Korea, HEDA 250 3D confocal Raman spectroscopy). The excitation power can be controlled by Raon-spec (Weve, South Korea), setting ND Filter value. In this research, ND Filter value was set to 100%, equivalent to 37mW. The Raman system was equipped with an 532nm laser, 1200 gr/mm grating, and a charged coupled device(CCD)-camera cooled to -40℃. With 1200gr/mm grating, possible spectra range was approximately 2000 at one time. To improve the accuracy of analysis, low frequency range and high frequency range was collected every 2hr respectively. Further description and reason for these data acquisition will be covered at 2.2 data analysis. The calibration for Raman system was conducted as matching $\boldsymbol{T_{2g}}$ mode of silicon wafer, $520 cm^{-1}$. The lateral solution can be calculated using The lateral and the depth resolution for 20× objective using in the air (n = 1.0) is limited by the diffraction limit[17].

$$\Delta_{\text{lat}} = \frac{0.61\lambda}{(N.A.)} = \frac{0.61 \cdot 532}{0.45} \sim 721\ nm \tag{2}$$

$$\Delta_{\text{dep}} = \pm\frac{4.4\lambda n}{2\pi(N.A.)^2} = \sim \pm 1840\ nm \tag{3}$$

The stage was remained same height to guarantee consistency of mapping area. Raman acquisition started 10min after

addition of water and mixing. Mapping area of 50×50 points was collected with 10 μm gap between points ($500\ \mu m \times 500\ \mu m$). Each point was collected with 0.8s of exposure time. The time for taking one map would take up to approximately 1hr due to stage shifting time. The initial 11hr of hydration was observed. The room temperature was maintained to 23℃ as possible to compare the data of previous study[16].

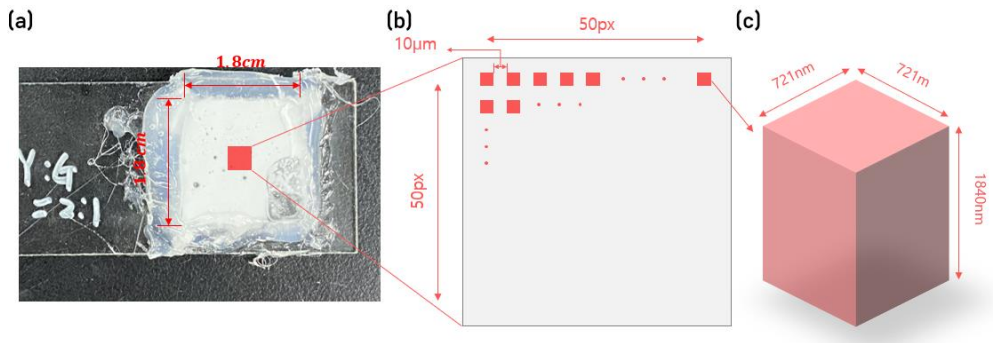

Figure 1 Sample Preparation for mapping and Raman Spectroscopy Specifications. (a) Sample mold developed for controlling water to cement ratio. Cement matrix is surrounded by glue gun sealing. (b) spatial summary of Raman data collection (c) laser spot lateral and depth resolution

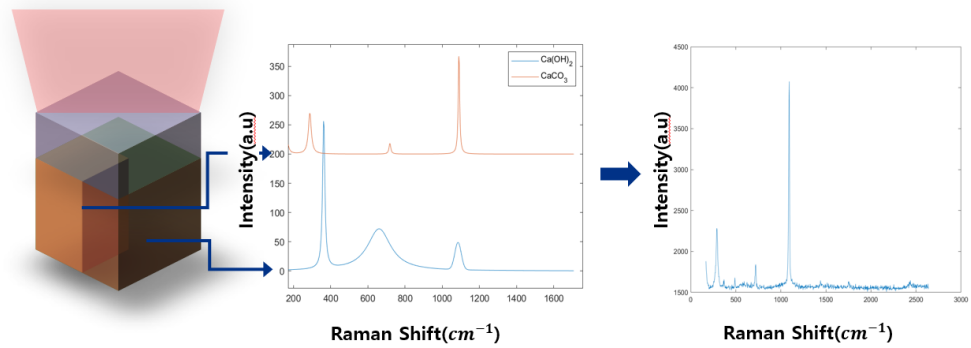

Figure 2 Graphical representation of laser spot acquiring heterogeneous material. Heterogeneous system may contain more than single material in a laser spot.

Table 1 Summary of the reported Raman shifts

Phase	AlO_4^{5-}		$Al(OH)_6$	SO_4^{2-}				Stretching $O-H$	Ref
	v_1	v_3		v_1	v_2	v_3	v_4		
Ye'elimite $C_4A_3\bar{S}$	482	645		993 s		1201	614		[18]
	521 m			991vs			616 w		[19]
Ettringite $C_6A\bar{S}_3H_{32}$			534	980 s			616 w	3458 b 3641 b	[18]
			549	990			615	3440 b 3638	[19]
			527,551	988	416,449	1087	581,605	3464 3624	[20]
			550	989	450	1114	610	3440 3637	[21]–[23]
Monosulfo aluminate			525	980 s		1114	616 w	3557sh 3619 b 3692 s	[18]
			532	982s/991 sh			615	3688	[19]
			531	983	450,396	1095	614	3688	[21]–[23]

* vw, very weak; s, strong; m, medium; b, broad; w, weak; sh, shoulder; vs,very strong.

2.3 Raman Data Analyses

2.3.1 Raman Data Acquisition

Expected main hydrates from ye'elimite hydration involve ettringite and AFm phases. Their reported characteristic peaks are at Table 1. Reported characteristic peaks of ye'elimite, ettringite and calcium sulfoaluminate are assigned primarily to SO_4^{2-} v_1 mode and their Raman shift positions range from 991~993 cm^{-1}, 980~990 cm^{-1} and 980~983 cm^{-1} respectively. Considering possible measurement error of Raman system with 1200gr is ~4 cm^{-1}, classification method only with one peak between those phases inevitably yield uncertainty in result. However, ye'elimite does not have any water stretching band while ettringite has unique water stretching band (3640 cm^{-1}). Thus, both lower frequency range and higher frequency range were recorded each time.

2.3.2 Raman Data Analyses formulation

The raw Raman data is 2-dimensional data with positional descriptor and its Raman intensity. Collected data in cementitious sample sometimes contains superposed data since multiple materials can be found in a single laser spot.(Figure.2) To enable analysis of

this data, basis analysis(BA) is adopted.[10] Generally, BA is conducted to generate linearly independent bases representing the data with their linear combinations. BA is an unsupervised method, meaning that the bases are computed without any labels. For deconvolution of mixed data and visualization, MATLAB was mainly used. Basic concept of basis analysis can be formulated like Eq. (4) below.

$$\mathrm{Y} = \begin{pmatrix} \alpha \\ \beta \\ \cdots \\ \omega \end{pmatrix} \begin{pmatrix} Basis_{\alpha} \\ Basis_{\beta} \\ \cdots \\ Basis_{\omega} \end{pmatrix} + \epsilon \; subject\ to\ \alpha + \beta + \cdots + \omega = 1 \tag{4}$$

The optimization of basis constant is conducted by minimizing R^2 value (Raw data to fitted data). Lsqlin function with interior-point algorithm in MATLAB was used.

2.3.3 Basis Dataset Construction

To enhance the accuracy in basis analysis, constructing exact basis dataset is at utmost importance. However, some of Raman spectrum are under change according to outer condition such as temperature, humidity and differences in equipment specification. Considering those features, there are no one ground truth basis spectrum in analysis.

If pure material is easily achievable, basis data was acquired

through Raman spectroscopy directly. To get basis spectrum, powders are placed on a slide glass and compressed for better data acquisition. Then, over 100 points were recorded for attaining reliable basis spectrum. The basis spectrum of which direct basis data collection is challenging such as AFm phases, data was assigned from hydrated sample.

Chapter 3. Results and Discussion

3.1 Basis Raman Spectra

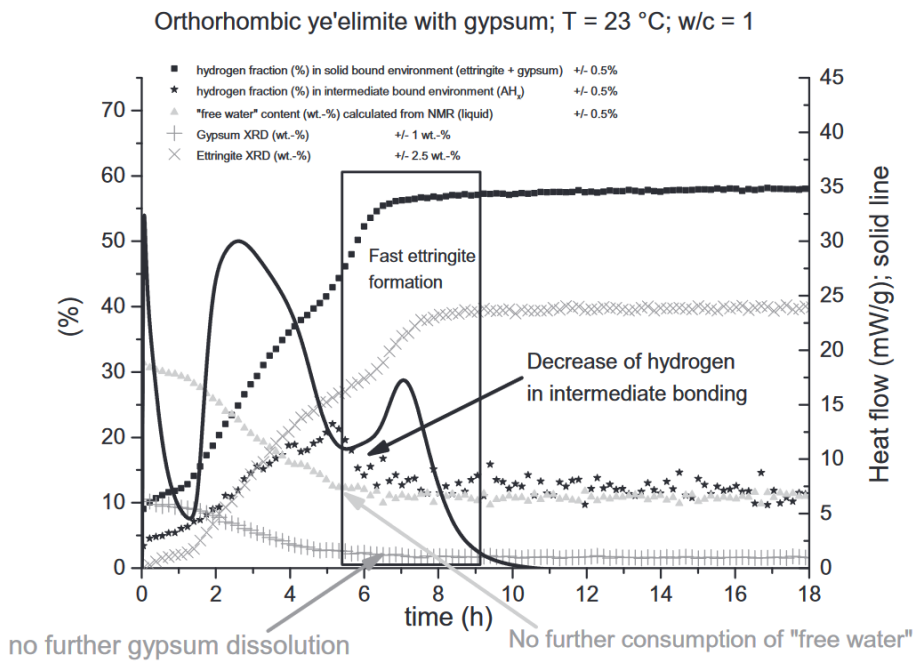

Figure 3 Heat flow curve, NMR results and XRD results determined for the reaction of orthorhombic ye'elimite with gypsum(T=23℃, w/c=1) [16]

Jansen's study[16] explained that additional ettringite formation without consumption of free water was enabled by water

supply from decomposition of aluminum hydroxide. Thus, our analysis focus on gypsum, water, ettringite and ye'elimite.

Basis spectrum used for analysis are illustrated in Figure. Basis spectrums for ye'elimite, gypsum and water are directly collected from their pure phases and for ettringite and aluminum hydroxide (amorphous and crystalline) are distinguished from hydrated ye'elimite paste. Basis spectrum of water is mainly composed of O−H stretching bond at 3408 cm^{-1}. The characteristic peak of gypsum, ye'elimite and ettringite is SO_4^{2-} v_1 mode; 1008 cm^{-1}, 990 cm^{-1} and 990 cm^{-1} respectively. They are corresponding with reported studies. For the case of amorphous aluminum hydroxide, basis spectrum modified from gibbsite Raman spectrum[20] were utilized; 538 cm^{-1}, 570cm^{-1}, 3355 cm^{-1},3427 cm^{-1}, 3525 cm^{-1} and 3617 cm^{-1} was used as collected from paste.

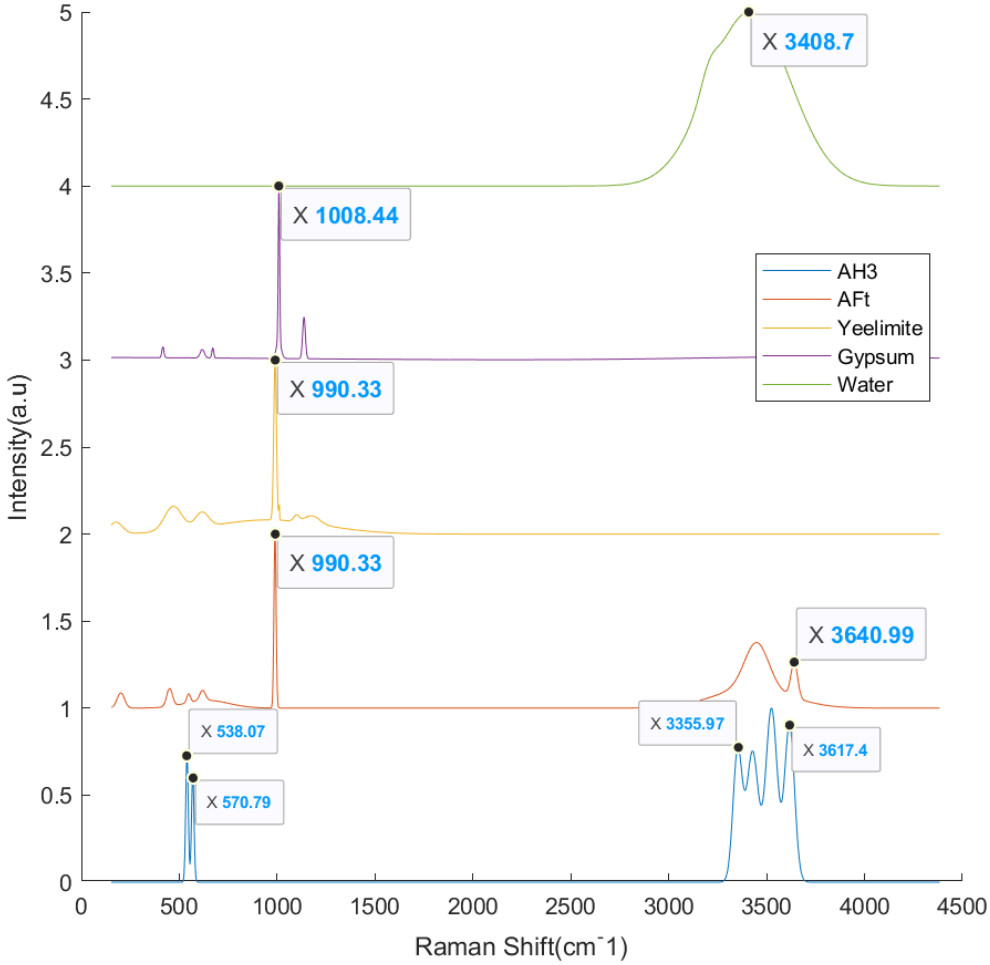

Figure 4 Plot of basis spectra used for analysis

3.2 Hydration Data Analyses

3.2.1 Average Raman Spectra Analysis

Phase transformation during ye'elimite hydration is tracked by plotting the average Raman spectra of the sampling area from 1 to 11 h. Initial paste was dominant with ye'elimite and gypsum that can be easily verified with strong Raman scatter SO_4^{2-} v_1 band (991cm^{-1} and 1008 cm^{-1}, respectively). Fast consumption of gypsum is observed between 1hr and 3hr. Consumption of ye'elimite is also expected but the peak position of SO_4^{2-} v_1 band change is too insignificant to judge based on only the average signal.

Thus, observing higher frequency is required. Peak position at 3409cm^{-1} and 3492 cm^{-1} are similar to peaks assigned to water stretching mode(v_1 and v_3 respectively) at previous study[21]. As those two peak intensities decreases, OH symmetric stretching of ettringite (3640 cm^{-1}) increases.

3.2.2 Visualization of Hydration Progress

The following figures (Fig.5−9) show the hydration progress of ye'elimite, water, ettringite and gypsum chronologically(1~11hr). First of all, decrease of ye'elimite(Fig.5) is illustrated until 7hr and then significant change are not found. A depletion of gypsum (Fig.6)

is considerably observed at first two mapping and from 5hr, reactivity of gypsum comparatively slows down. Similarly, the decrease of water(Fig.7) at overall map is dominant until 5hr. The image after 5hr mapping seemed to be stationary. According to calorimetry result of jansen's, additional ettringite formation was recorded after little break after initial ettringite formation. Consumption of gypsum and free water was only significant at first ettringite formation reaction. This trend is similarly approved with Raman imaging results. The Raman image of ettringite shows consistent formation through all observation time. An ettringite formation without consumption of free water can be described by Raman image change of aluminum hydroxide. The intensity of aluminum hydroxide dwindles when the ettringite are created without the decrease of water. This phenomenon is clarified by summarizing in a graph.

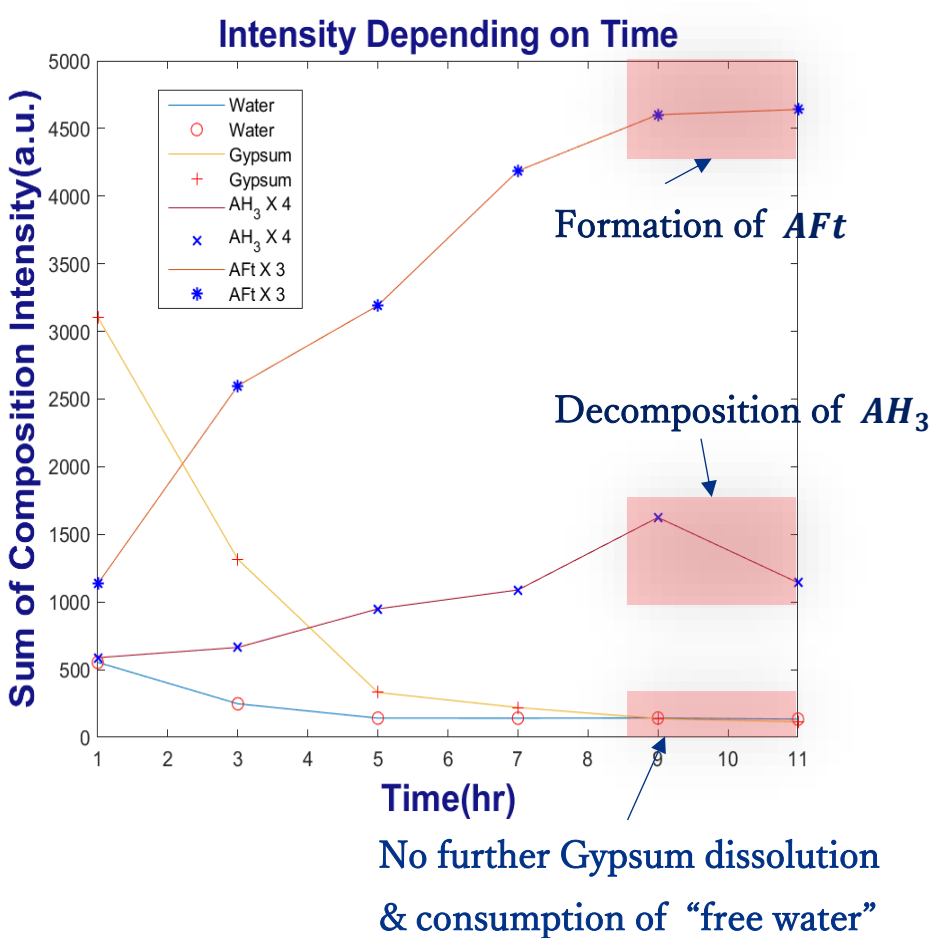

Figure 5 Raman intensity curve, Raman intensity of each phases are plotted. Aluminum hydroxide and ettringite value was multipled to facilitate comparison. Intensity is under arbitrary unit since their basis spectrum is not normalized.

The graph (Fig. 5) shows the sum of composition intensity. After 5hr, gypsum and water consumption are slowed down. The sum of aluminum hydroxide intensity at 9hr to 11hr decreased which means decomposition of aluminum hydroxide. This released water to form additional ettringite.

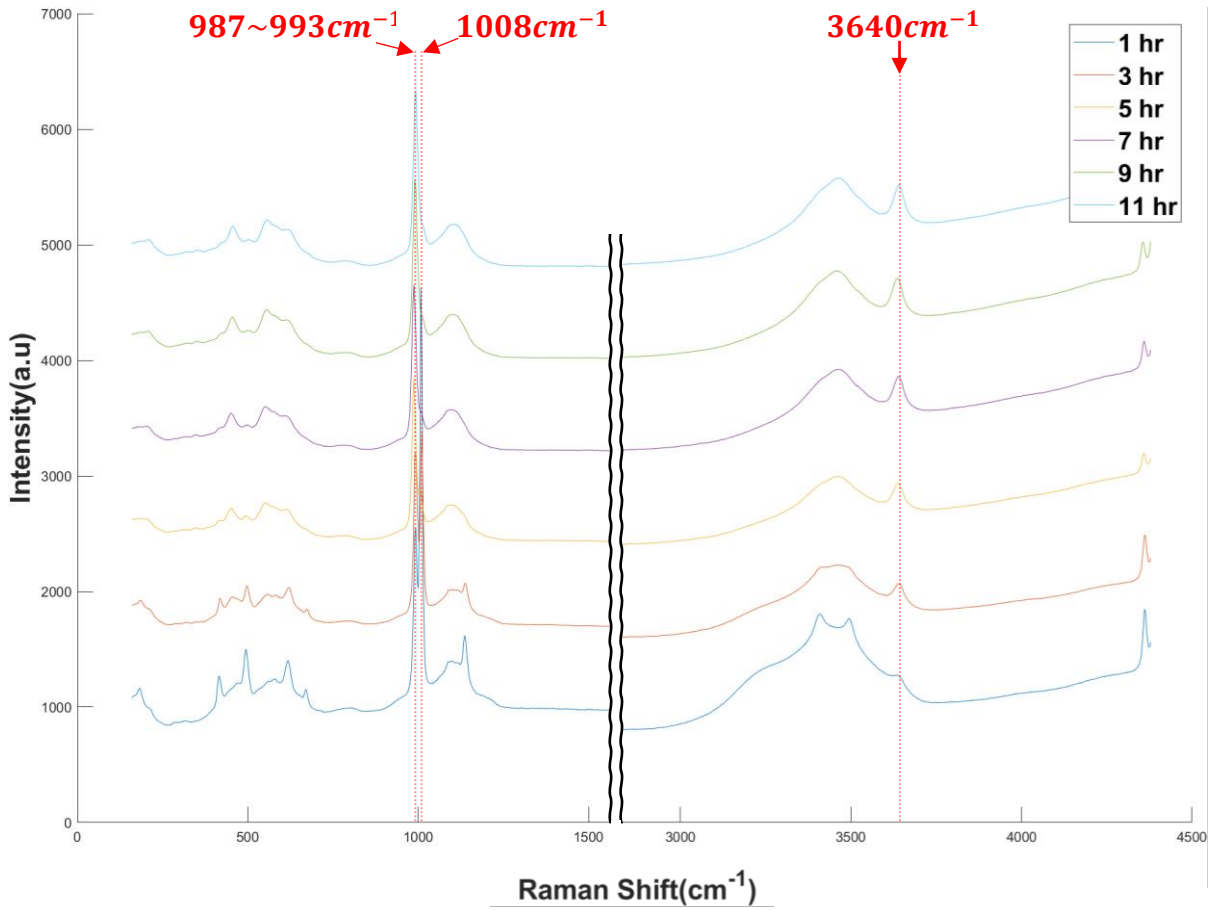

Figure 6 Average Raman spectra during the early stage ye'elimite hydration (1~11hr)

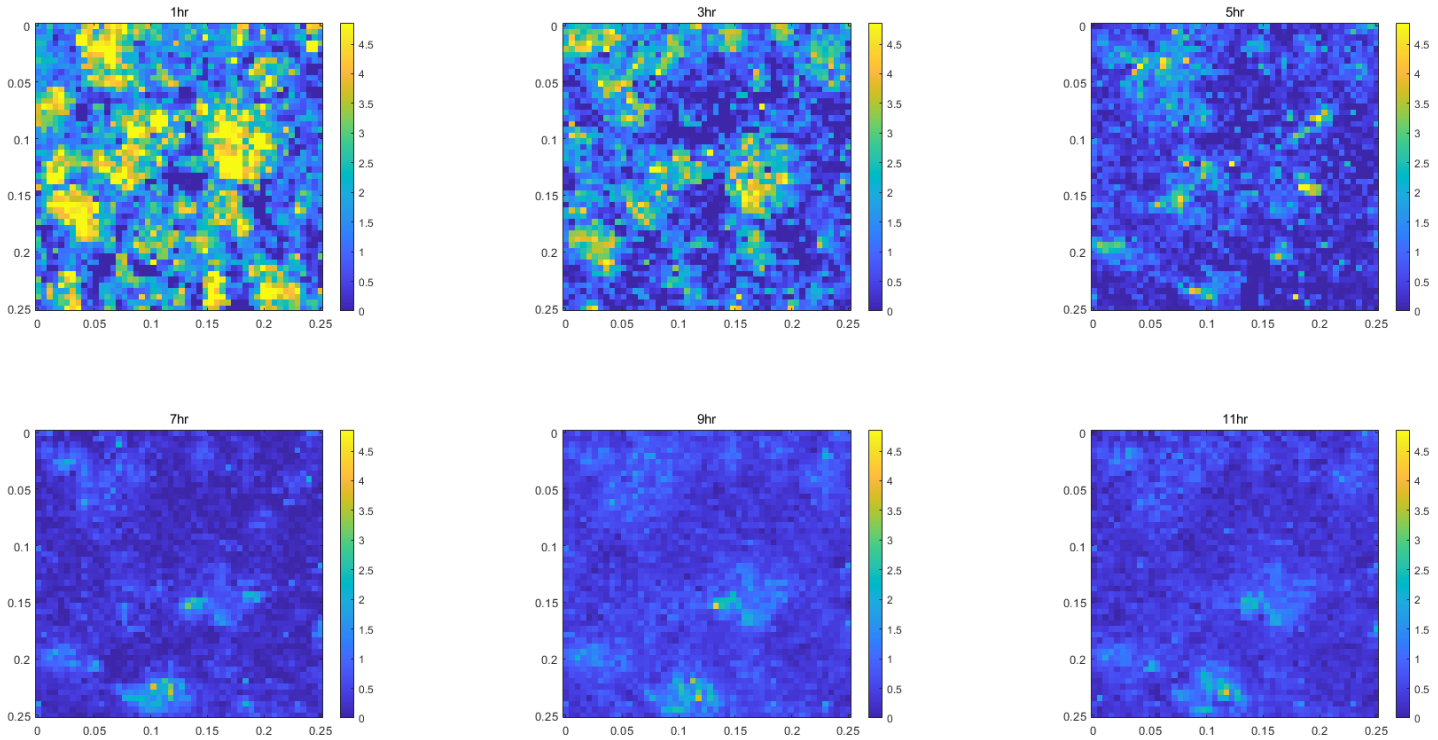

Figure 7 Raman intensity of ye'elimite mapping. Color bar shows Raman intensity.

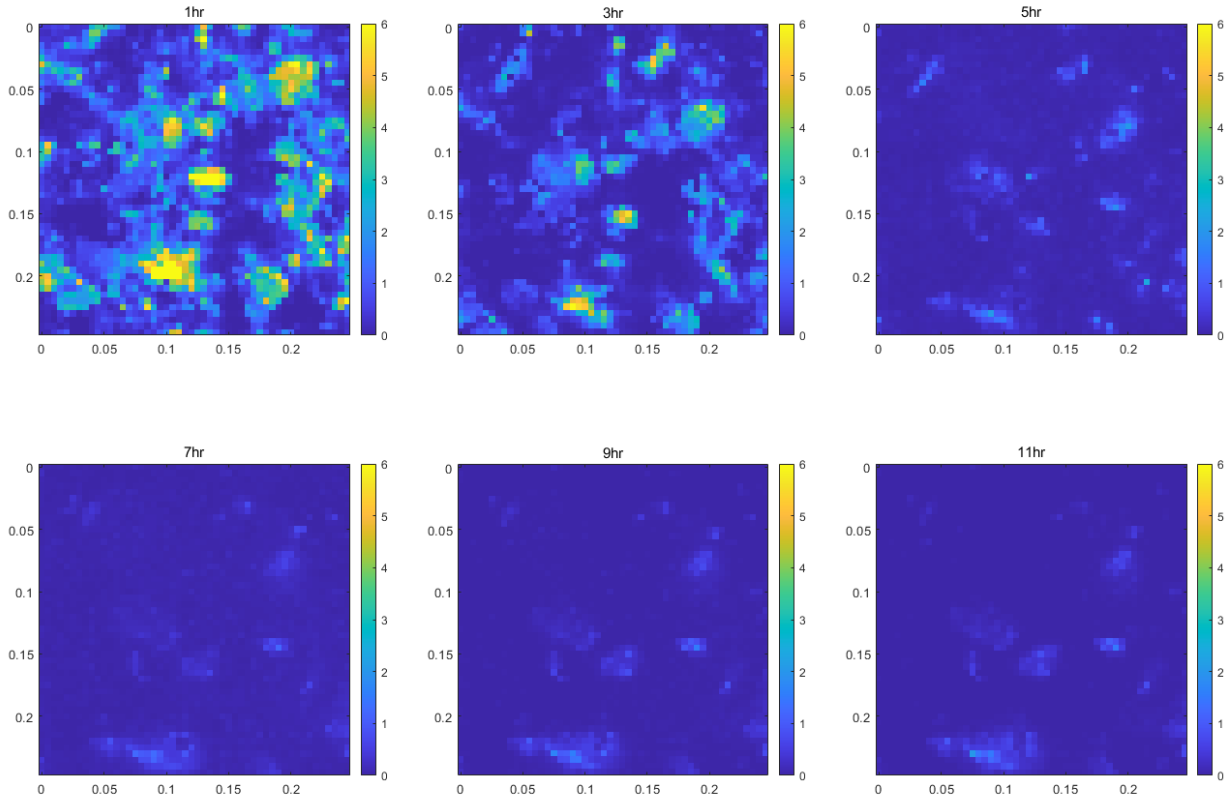

Figure 8 Raman intensity of gypsum mapping. Color bar shows Raman intensity.

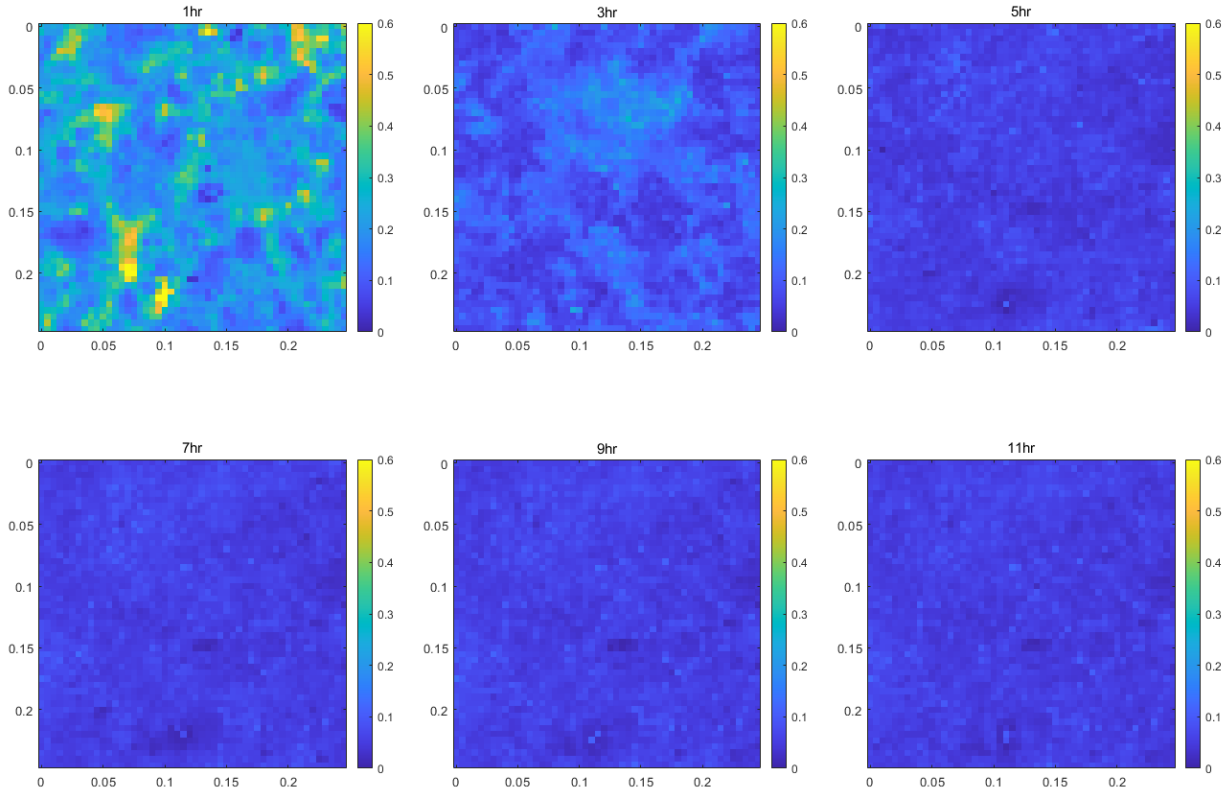

Figure 9 Raman intensity of water mapping. Colorbar shows Raman intensity.

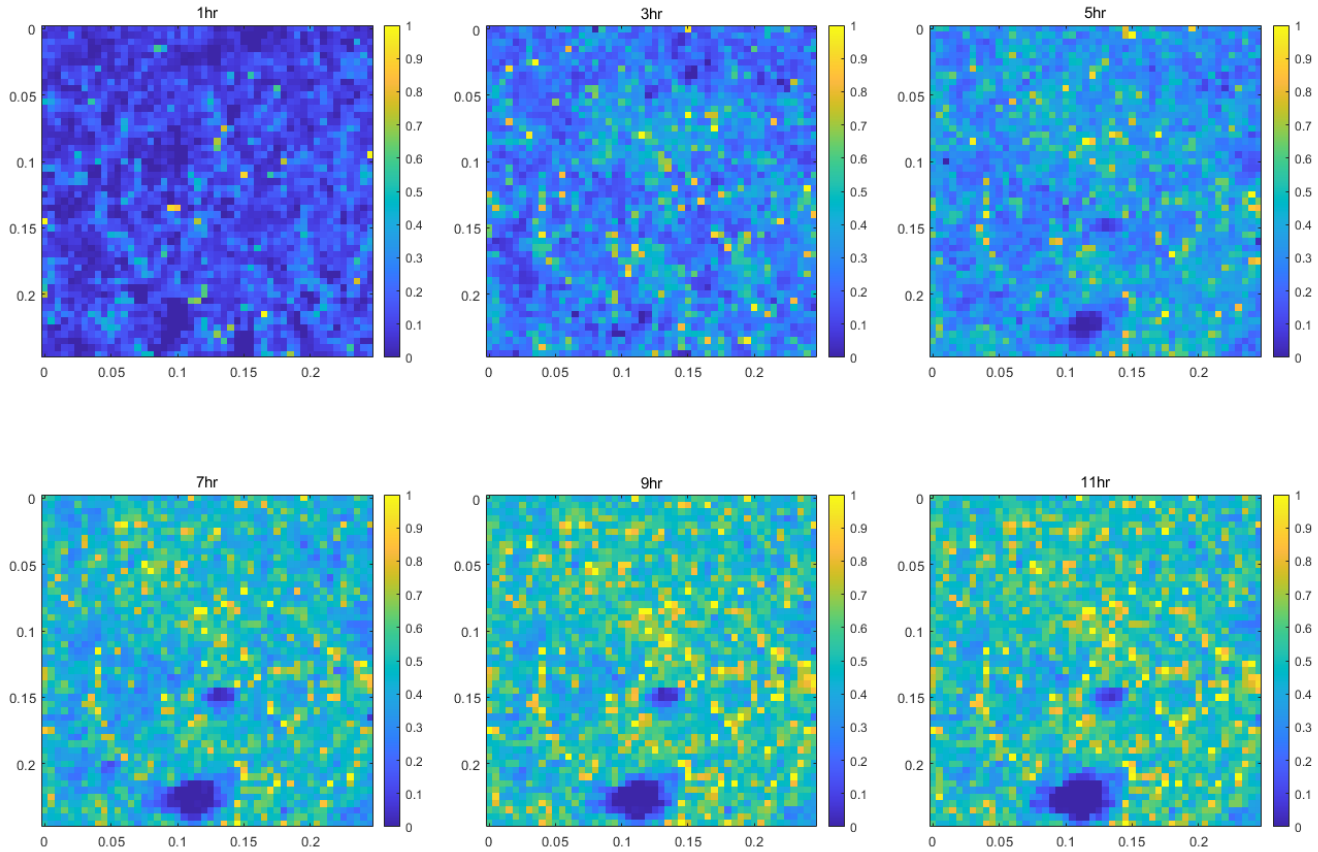

Figure 10 Raman intensity of ettringite mapping. Colorbar shows Raman intensity.

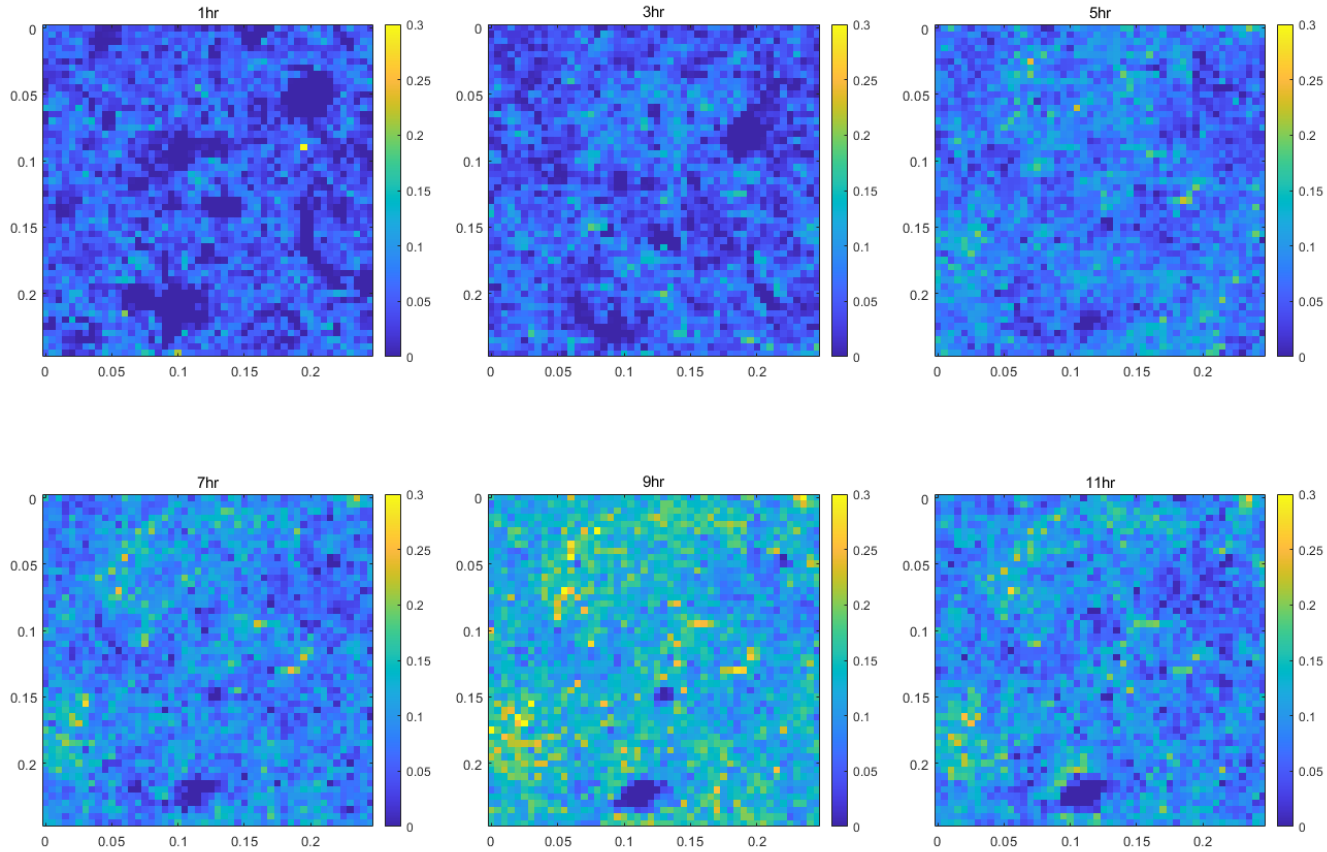

Figure 11 Raman intensity of aluminum hydroxide mapping. Colorbar shows Raman intensity.

water

Chapter 4. Limitation and Further research

In this study, we enabled disability to setting water to ratio freely for in-situ Raman imaging. However, it has temporal and spatial resolution error. This problem could be solved with adopting 600mm/g grating. Theoretically, 600mm/g grating has two times wider range than 1200mm/g grating. This will decrease data acquisition time in half, removing procedure of collecting lower frequency and higher frequency respectively. It means spatial resolution can be doubled if temporally dense mapping is not required. However, 600mm/g grating inherently has larger spectral resolution error in Raman peak positions which can be up to $8cm^{-1}$. Thus, grating selection should be considered depending on which cementitious material will be focused. Quantitative analysis that could not be carried out due to the limited spatial resolution can be carried out.

And also, securing statistical effectiveness is a challenge that Raman spectroscopy should overcome. Even though this study had performed large in-situ scan area among the reported studies so far, still small area($500\,\mu m \times 500\,\mu m$) compared to cement surface ($1.8cm \times 1.8cm$) is cautiously addressed to conclude correctly.

Furthermore, even though basis analysis method can distinguish between substrate (slide glass) and phases of our interest, the more robust method of Raman spectrum interpretation should be needed. Each peak has their own positions, intensity, and width containing a variety of information about the atomic structure in local area. These can be analyzed with atomic simulation such as Density Functional Theory(DFT) and Molecular Dydamics(MD). If further research about expanding our knowledge of Raman spectrum, more meaningful analysis about atomic structure change in hydration can be conducted.

Also, phase quantification will facilitate tracking the change of hydration kinetics. This is fundamental to analyze phase transition quantitively. The example of ongoing phase quantification and transition anlaysis is conducted with ye'elimite hydration without calcium sulfate source such as gypsum. The mapping result is listed below.

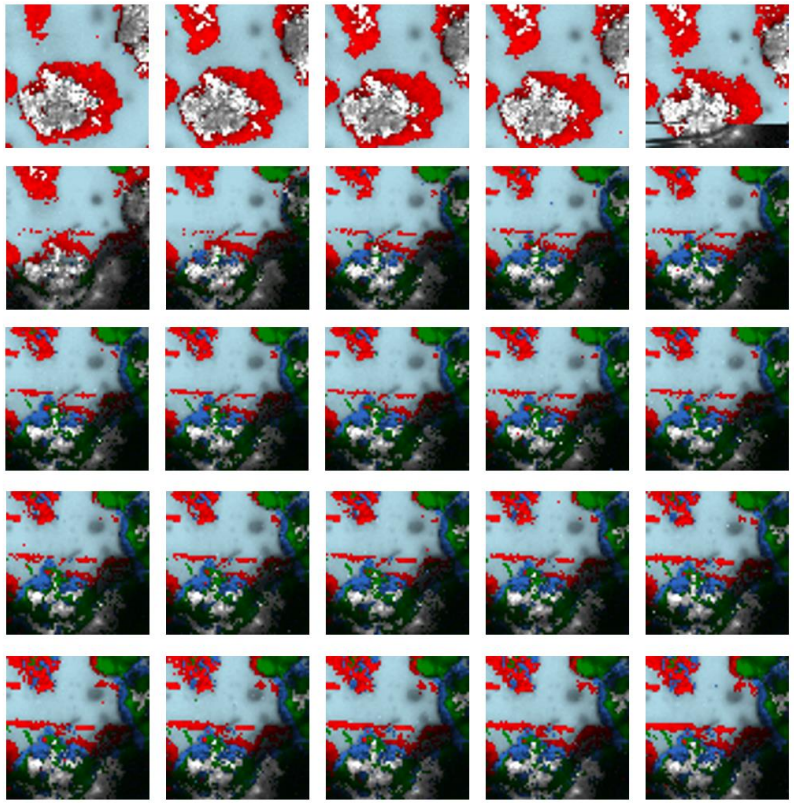

1	2	3	4	5
6	7	8	9	10
11	12	13	14	15
16	17	18	19	20
21	22	23	24	25

Figure 12 Mapping and phase quantification of ye'elimite hydration from 1hr to 25 hr. Raman map is colored with green (AFm), blue (AH3), red(ettringite), sky blue(water), and white(ye'elimite). Temporal order of the Raman map is following the matrix on the right.

Chapter 5. Conclusion

This paper shows the method to perform in-situ Raman imaging with controlling water to cement ratio, which is one of the most important factors to cement hydration. Raman spectroscopy can be useful to track hydration of cementitious phases. Complex phenomena like water supply by aluminum hydroxide decomposition and consequent additional ettringite formation were successfully recorded and analyzed. An important aspect is the investigation of the local environment of the anionic species and the hydrogen bond network through the measurement of the water and hydroxyl stretchings. Not only this method saves the time to analyze cement hydration kinetics, but also enables spatial characterization of heterogeneous and amorphous constituent phase in various time span including early age.

Bibliography

[1] M. S. Imbabi, C. Carrigan와/과S. McKenna, “Trends and developments in green cement and concrete technology”, *Int. J. Sustain. Built Environ.*, vol 1, 호 2, pp 194–216, 12 2012, doi: 10.1016/j.ijsbe.2013.05.001.

[2] W. Shen, L. Cao, Q. Li, W. Zhang, G. Wang와/과C. Li, “Quantifying CO2 emissions from China’s cement industry”, *Renew. Sustain. Energy Rev.*, vol 50, pp 1004–1012, 10 2015, doi: 10.1016/j.rser.2015.05.031.

[3] C. W. Hargis, B. Lothenbach, C. J. Müller와/과F. Winnefeld, “Carbonation of calcium sulfoaluminate mortars”, *Cem. Concr. Compos.*, vol 80, pp 123–134, 7 2017, doi: 10.1016/j.cemconcomp.2017.03.003.

[4] “Cement Statistics and Information | U.S. Geological Survey”. https://www.usgs.gov/centers/national-minerals-information-center/cement-statistics-and-information (접근된 2023년 1월 26일).

[5] E. Gartner, “Industrially interesting approaches to ‘low-CO2’ cements”, *Cem. Concr. Res.*, vol 34, 호 9, pp 1489–1498, 9 2004, doi: 10.1016/j.cemconres.2004.01.021.

[6] T. Hanein, J.-L. Galvez-Martos와/과M. N. Bannerman, “Carbon footprint of calcium sulfoaluminate clinker production”, *J. Clean. Prod.*, vol 172, pp 2278–2287, 1 2018, doi: 10.1016/j.jclepro.2017.11.183.

[7] K. L. Scrivener, V. M. John와/과E. M. Gartner, “Eco-efficient cements: Potential economically viable solutions for a low-CO2 cement-based materials industry”, *Cem. Concr. Res.*, vol 114, pp 2–26, 12 2018, doi: 10.1016/j.cemconres.2018.03.015.

[8] D. Xue, P. V. Balachandran, J. Hogden, J. Theiler, D. Xue와/과T. Lookman, “Accelerated search for materials with targeted properties by adaptive design”, *Nat. Commun.*, vol 7, 호 1, p 11241, 4 2016, doi: 10.1038/ncomms11241.

[9] J. Toporski, T. Dieing와/과O. Hollricher, *Confocal Raman Microscopy*, vol 66. Springer, 2018.

[10] H.-C. Loh, H.-J. Kim, F.-J. Ulm와/과A. Masic, “Time-Space-Resolved Chemical Deconvolution of Cementitious Colloidal Systems Using Raman Spectroscopy”, *Langmuir*, vol 37, 호 23, pp 7019–7031, 6 2021, doi: 10.1021/acs.langmuir.1c00609.

[11] F. Winnefeld와/과S. Barlag, “Influence of calcium sulfate and calcium hydroxide on the hydration of calcium sulfoaluminate clinker”, *Zkg Int*, vol 62, 호 12, pp 42–53, 2009.

[12] F. Winnefeld와/과S. Barlag, “Calorimetric and

thermogravimetric study on the influence of calcium sulfate on the hydration of ye'elimite", *J. Therm. Anal. Calorim.*, vol 101, 호 3, pp 949–957, 2010.
[13] I. A. Chen, C. W. Hargis와/과M. C. Juenger, "Understanding expansion in calcium sulfoaluminate–belite cements", *Cem. Concr. Res.*, vol 42, 호 1, pp 51–60, 2012.
[14] L. Zhang, M. Su와/과Y. Wang, "Development of the use of sulfo-and ferroaluminate cements in China", *Adv. Cem. Res.*, vol 11, 호 1, pp 15–21, 1999.
[15] H.-M. Ludwig와/과W. Zhang, "Research review of cement clinker chemistry", *Cem. Concr. Res.*, vol 78, pp 24–37, 2015.
[16] D. Jansen, A. Spies, J. Neubauer, D. Ectors와/과F. Goetz-Neunhoeffer, "Studies on the early hydration of two modifications of ye'elimite with gypsum", *Cem. Concr. Res.*, vol 91, pp 106–116, 1 2017, doi: 10.1016/j.cemconres.2016.11.009.
[17] S. Gamsjaeger기타, "Cortical bone composition and orientation as a function of animal and tissue age in mice by Raman spectroscopy", *Bone*, vol 47, 호 2, pp 392–399, 8 2010, doi: 10.1016/j.bone.2010.04.608.
[18] D. Torréns-Martín, L. Fernández-Carrasco, S. Martínez-Ramírez, J. Ibáñez, L. Artús와/과T. Matschei, "Raman Spectroscopy of Anhydrous and Hydrated Calcium Aluminates and Sulfoaluminates", *J. Am. Ceram. Soc.*, vol 96, 호 11, pp 3589–3595, 11 2013, doi: 10.1111/jace.12535.
[19] D. Gastaldi, E. Boccaleri, F. Canonico와/과M. Bianchi, "The use of Raman spectroscopy as a versatile characterization tool for calcium sulphoaluminate cements: a compositional and hydration study", *J. Mater. Sci.*, vol 42, 호 20, pp 8426–8432, 8 2007, doi: 10.1007/s10853-007-1790-8.
[20] H. D. Ruan, R. L. Frost와/과J. T. Kloprogge, "Comparison of Raman spectra in characterizing gibbsite, bayerite, diaspore and boehmite", *J. Raman Spectrosc.*, vol 32, 호 9, pp 745–750, 9 2001, doi: 10.1002/jrs.736.
[21] P. Prasad, A. Pradhan와/과T. Gowd, "In situ micro-Raman investigation of dehydration mechanism in natural gypsum", *Curr. Sci.*, pp 1203–1207, 2001.

Abstract in Korean

본 논문에서는 수화과정을 포함하는 구조재료 바인더 연구를 위하여 실시간 라만 이미징 분석기법을 개발하였다. 기존에 보고된 라만 분광법 실험은 샘플의 양생 조건 및 촬영조건에 있어서 실제 시멘트계 재료의 수화과정과 다른 점이 많았다. 본 연구에서는 이러한 한계를 극복하기 위해 샘플을 커버글라스와 글루건을 활용하여 밀봉하여 표면의 오염과 측정광으로 인한 표면 수분 증발을 방지하고 시멘트 수화과정에 중요한 요소인 물-시멘트 비를 일정하게 조정한 상태에서의 실시간 시멘트 수화과정을 측정할 수 있었다. 이러한 조건에서 측정된 데이터를 해석을 하기 위해서 기저 분석법(Basis analysis)을 도입하여 커버글라스로 인해 발생하는 라만 스펙트럼을 분리하여 측정 대상인 시멘트계 재료의 화학적 변화를 실시간으로 관측할 수 있었다.

라만 이미징 기술과 본 방법의 분석 잠재능력을 평가하기 위해 석고를 첨가한 일리마이트 결정의 수화과정을 촬영하고 분석하였다. 기존의 XRD와 NMR로 분석한 논문과 달리 비정질 수산화알루미늄을 포함한 기존 방법으로는 분석이 어려운 상 또한 명확히 발견되었다. 또한, 라만 분광기를 이용하여 많은 노력과 시간을 절감하면서 실시간 수화 분석이 가능하였다. 추가로, XRD와 SEM과 같은 기존의 방법으로 불가능한 실시간 수화과정의 시공간적 해석이 가능했으며 수산화알루미늄이 분해되는 곳에 추가적인 에트린가이트 형성이 일어나는 것을 공간적으로 확인했다. 개발된 본 방법은 극초기를 포함한 다양한 시간대에서 발생하는 복잡한 구조재료의 수화과정, 특히 비균질 또는 비정질 상의 특징과 시공간적 분포에 관한 정보를 통해 수화현상을 정확히 분석할 수 있는 기법으로 활용될 수 있을 것으로 기대된다.